




Article

# ZFH3 Promotes the Proliferation and Tumor Growth of ER-Positive Breast Cancer Cells Likely by Enhancing Stem-Like Features and *MYC* and *TBX3* Transcription

Ge Dong<sup>1</sup>, Gui Ma<sup>1</sup>, Rui Wu<sup>2</sup>, Jinming Liu<sup>1</sup>, Mingcheng Liu<sup>1,2</sup>, Ang Gao<sup>1</sup>, Xiawei Li<sup>1,2</sup>, Jun A<sup>1,2</sup>, Xiaoyu Liu<sup>2</sup>, Zhiqian Zhang<sup>2</sup> , Baotong Zhang<sup>3</sup> , Liya Fu<sup>1</sup> and Jin-Tang Dong<sup>2,\*</sup> 

<sup>1</sup> Department of Genetics and Cell Biology, College of Life Sciences, Nankai University, 94 Weijin Road, Tianjin 300071, China; 1120160366@mail.nankai.edu.cn (G.D.); gma24@wisc.edu (G.M.); 2120171046@mail.nankai.edu.cn (J.L.); 1120170388@mail.nankai.edu.cn (M.L.); agao22@wisc.edu (A.G.); 1120180410@mail.nankai.edu.cn (X.L.); 1120170387@mail.nankai.edu.cn (J.A.); fuchu12@nankai.edu.cn (L.F.)

<sup>2</sup> Department of Human Cell Biology and Genetics, School of Medicine, Southern University of Science and Technology, 1088 Xueyuan Blvd, Shenzhen 518055, China; wur@sustech.edu.cn (R.W.); liuxy9@sustech.edu.cn (X.L.); zhangzq@sustc.edu.cn (Z.Z.)

<sup>3</sup> Emory Winship Cancer Institute, Department of Hematology and Medical Oncology, Emory University School of Medicine, 1365-C Clifton Road, Atlanta, GA 30322, USA; baotong.zhang@emory.edu

\* Correspondence: dongjt@sustech.edu.cn

Received: 27 October 2020; Accepted: 12 November 2020; Published: 18 November 2020



**Simple Summary:** Breast cancer is a common malignancy, but the understanding of its cellular and molecular mechanisms is limited. The ZFH3 transcription factor regulates mammary epithelial cells' proliferation and differentiation by interacting with estrogen and progesterone receptors. Both these receptors play crucial roles in breast cancer development, but whether ZFH3 also impacts breast cancer is unknown. In this study, the authors aim to determine if ZFH3 promotes breast cancer cells' proliferation and tumor growth and explore the underlying cellular and molecular mechanisms. Higher ZFH3 expression is associated with worse patient survival in breast cancer, ZFH3 promotes the proliferation and tumor growth of breast cancer cells, and several breast cancer stem cell factors appear to be involved in the role of ZFH3 in breast cancer growth. The findings suggest that ZFH3 is a novel oncogenic molecule promoting breast cancer development. Such a molecule could provide novel opportunities for the treatment of breast cancer.

**Abstract:** Breast cancer is a common malignancy, but the understanding of its cellular and molecular mechanisms is limited. ZFH3, a transcription factor with many homeodomains and zinc fingers, suppresses prostatic carcinogenesis but promotes tumor growth of liver cancer cells. ZFH3 regulates mammary epithelial cells' proliferation and differentiation by interacting with estrogen and progesterone receptors, potent breast cancer regulators. However, whether ZFH3 plays a role in breast carcinogenesis is unknown. Here, we found that ZFH3 promoted the proliferation and tumor growth of breast cancer cells in culture and nude mice; and higher expression of ZFH3 in human breast cancer specimens was associated with poorer prognosis. The knockdown of ZFH3 in ZFH3-high MCF-7 cells decreased, and ZFH3 overexpression in ZFH3-low T-47D cells increased the proportion of breast cancer stem cells (BCSCs) defined by mammosphere formation and the expression of CD44, CD24, and/or aldehyde dehydrogenase 1. Among several transcription factors that have been implicated in BCSCs, MYC and TBX3 were transcriptionally activated by ZFH3 via promoter binding, as demonstrated by luciferase-reporter and ChIP assays. These findings suggest that ZFH3 promotes breast cancer cells' proliferation and tumor growth likely by enhancing BCSC features and upregulating MYC, TBX3, and others.

**Keywords:** ZFHX3; breast cancer; MYC; TBX3; cancer cells stemness

---

## 1. Introduction

Breast cancer is a common malignancy among women [1]. Estrogen receptor alpha (ER) signaling is the defining and driving force in most breast cancers, and selective ER modulator (SERM) therapy is widely used to treat breast cancer. While other signaling pathways also modulate breast carcinogenesis, the expression status of ER, progesterone receptor (PR), human epidermal growth factor receptor 2 (HER2), and the Ki67 proliferation marker stratify breast cancers into several subtypes, such as luminal A (ER<sup>+</sup> and/or PR<sup>+</sup>/HER2<sup>-</sup> and low Ki67 index), luminal B (ER<sup>+</sup> and/or PR<sup>+</sup> and higher Ki67 index), triple-negative (ER<sup>-</sup>/PR<sup>-</sup>/HER2<sup>-</sup> with higher Ki67 index), and HER2 enriched [2,3]. Although most breast cancers are luminal tumors and a higher Ki67 index distinguishes luminal B from luminal A tumors [4], ER<sup>+</sup>/PR<sup>-</sup> luminal tumors have a unique gene expression signature. They are less responsive than ER<sup>+</sup>/PR<sup>+</sup> tumors to SERM therapy [5]. While PR can be transcriptionally induced by ER and PR can cause or promote breast carcinogenesis [6–8], PR also has unique ER-independent functions in luminal breast cancer [7,9]. PR can even be a tumor suppressor in ER-mediated tumor growth of breast cancer [10]. Therefore, it is still an important task to understand the molecular modulators of breast cancer.

ZFHX3 (zinc finger homeobox 3), also known as ATBF1, encodes a large transcription factor with four homeodomains and 23 zinc finger motifs. It has two different transcripts, ATBF1-A and ATBF1-B, with the former having extra residues in the N-terminus [11,12]. ZFHX3 has diverse functions in normal and diseased cells. For example, while ZFHX3 induces neuronal differentiation in both cultured cells and developing mouse brains [11–13], it also regulates mammary gland development at different stages via different mechanisms. In pubertal mouse mammary glands, *Zfhx3* inhibits cell proliferation and ductal elongation and bifurcation [14]. However, during reproduction, *Zfhx3* promotes mammary epithelial cell proliferation, side branching, alveologenesis, and lactogenic differentiation [15,16]. Although higher levels of *ZFHX3-A* mRNA in breast cancer cells are associated with better prognosis, such as smaller tumor size and reduced lymph node metastasis in breast cancer [17], *ZFHX3* is transcriptionally upregulated by both the estrogen/ER and progesterone (Pg)/PR signaling pathways via the binding of ER and PR, respectively, to the *ZFHX3* promoter [15,18,19]. Combining ER and PR's roles in breast cancer and their interactions with *ZFHX3* [14,15,20], it is likely that *ZFHX3* plays a role in breast carcinogenesis. However, this hypothesis has not been tested.

In this study, we examined the role of *ZFHX3* in breast cancer cells' proliferation and tumor growth using in vitro and in vivo models. We also explored how *ZFHX3* modulates breast cancer growth by focusing on breast cancer stem cell (BCSC) features and *ZFHX3*'s downstream target genes. We found that *ZFHX3* promotes breast cancer cell proliferation and tumor growth, and the underlying cellular and molecular mechanisms involve BCSC-like features and transcriptional activation of *MYC* and *TBX3*. These findings suggest a regulatory role of *ZFHX3* in breast carcinogenesis and provide a potential therapeutic opportunity for breast cancer therapy.

## 2. Results

### 2.1. *ZFHX3* Enhances Breast Cancer Cell Proliferation and Tumorigenicity

To test whether *ZFHX3* modulates breast cancer cell proliferation and tumorigenicity, we first surveyed the levels of endogenous *ZFHX3* expression in 5 breast cell lines by western blotting. Among them, MCF-7 had higher expression of *ZFHX3*, while T-47D, BT-474, and MDA-MB-231 expressed *ZFHX3* at lower levels (Figure S1), which is consistent with a previous study [20]. In MCF-7 cells, *ZFHX3* silencing inhibited cell growth (Figure 1a). Consistently, the 3-D colony formation assay showed that both the number and size of spheres were decreased in *ZFHX3* silencing (Figure 1b).

In T-47D cells, which express less ZFH3, ectopic expression of ZFH3 significantly promoted cell proliferation (Figure 1c) and increased both the size and number of spheres in the Matrigel assay (Figure 1d). ZFH3 thus plays a promoting role in breast cancer cell proliferation in vitro.

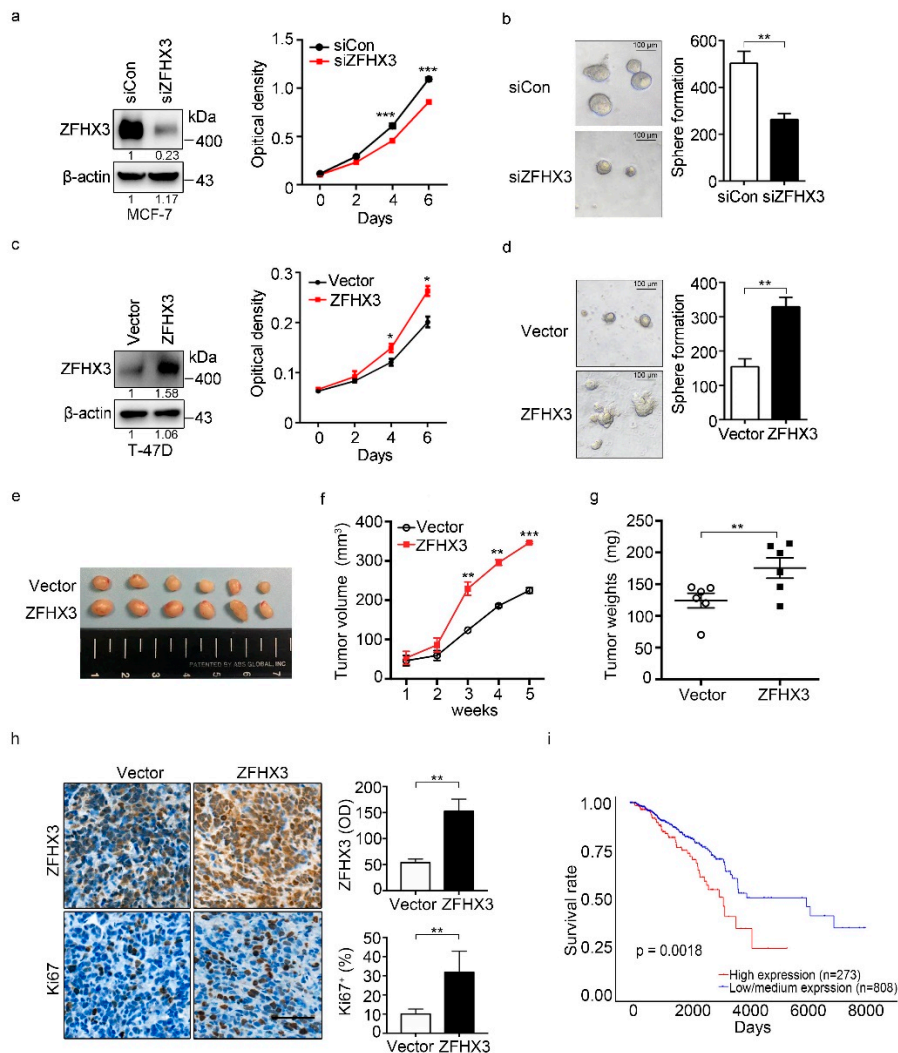


**Figure 1.** ZFH3 enhances colony formation and tumorigenicity of ER<sup>+</sup> breast cancer cells. (a,b) ZFH3 silencing by RNAi inhibited colony formation in 2D culture (a), as determined by the sulforhodamine B (SRB) assay, and sphere formation in Matrigel (b), as indicated by representative images of spheres (left) and the numbers of spheres with a diameter >75 μm (right) in MCF-7 cells. siCon, control siRNA; siZFHX3, siRNA against ZFH3. (c,d) Ectopic expression of ZFH3 promoted colony formation in the 2D SRB assay (c) and 3D sphere formation in Matrigel (d) in T-47D cells. (e–g) ZFH3 expression in T-47D cells also promoted their subcutaneous tumor formation in nude mice, as indicated by tumor images (e), tumor growth curve (f), and tumor weight (g). (h) Enhanced tumor growth by ZFH3 was accompanied by increased cell proliferation, as indicated by representative images of IHC staining of ZFH3, Ki67 in xenograft tumors, and the quantification of ZFH3-positive cells (up), Ki67-positive cells (down). Scale bar, 50 μm. (i) Higher mRNA levels of ZFH3 are associated with worse survival in patients with breast cancer in the TCGA database, as analyzed by survival analysis. \*  $p < 0.05$ ; \*\*  $p < 0.01$ ; \*\*\*  $p < 0.001$ . Ratios of protein band intensities to those of their loading controls, with the control sample's normalized to 1, are shown under bands in western blots (a,c). Uncropped western blot images are available in Supplementary Figure S7.

To further test how ZFH3 impacts breast cancer growth, we injected T-47D cells with ectopic expression of ZFH3 into the mammary fat pads of nude mice and analyzed their tumorigenicity.

ZFHX3 overexpression in T-47D cells significantly increased tumor volume, tumor weight, and the Ki67 proliferation index when compared with control groups (Figure 1e–h). Consistently, ZFHX3 silencing in MCF-7 cells significantly decreased tumor growth and cell proliferation (Figure S2). Results from the in vivo model further indicate that ZFHX3 increases xenograft tumor growth of breast cancer cells.

We further evaluated the role of ZFHX3 in breast cancer by comparing breast cancers with lower and higher ZFHX3 mRNA expression levels for patient survival using data from the Cancer Genome Atlas (TCGA) database [21,22]. Patients with lower ZFHX3 expression in their tumors had longer overall survival time than those with higher ZFHX3 in their tumors (Figure 1i,  $p = 0.0018$ ). Taking these findings together, we conclude that ZFHX3 promotes breast cancer growth, at least in a subset of patients.

## 2.2. ZFHX3 Is Involved in the Maintenance of BCSC-Like Features

ZFHX3 has been implicated in mammary gland stemness [19], and BCSCs are proposed to drive breast cancer initiation and progression. We thus sought to determine whether ZFHX3 affects BCSC traits. High expression of CD44 and low expression of CD24 (CD44<sup>+</sup>/CD24<sup>-</sup>) are useful for identifying and isolating the cells with stem-like properties in normal mammary tissues and breast carcinomas [23–25]. We first compared the expression patterns of ZFHX3 and several genes involved in BCSCs between CD44<sup>+</sup>/CD24<sup>-</sup> and CD44<sup>-</sup>/CD24<sup>+</sup> populations of MCF10A cells in the GSE15192 dataset [26]. Interestingly, the CD44<sup>+</sup>/CD24<sup>-</sup> population expressed higher levels of ZFHX3, along with multiple pluripotency factors such as MYC, TBX3, SOX2, NANOG, and OCT4, than the CD44<sup>-</sup>/CD24<sup>+</sup> population (Figure S3), suggesting a correlation between ZFHX3 expression and mammary cell stemness.

We then examined the effect of ZFHX3 expression on self-renewal potential, as indicated by the mammosphere forming capability, and the proportions of ALDH<sup>+</sup> and CD44<sup>+</sup>/CD24<sup>-</sup> cells. In MCF-7 cells, ZFHX3 silencing reduced the mammosphere formation efficiency and decreased the population size of ALDH<sup>+</sup>/CD44<sup>+</sup>/CD24<sup>-</sup> cells (Figure 2a–c). Similarly, silencing ZFHX3 in MCF-7 cells with two shRNAs, whose knockdown effects were confirmed by western blotting (Figure S4a), decreased mammosphere formation (Figure S4b) and reduced the ALDH<sup>+</sup> population when compared to control cells (Figure S4c). Conversely, ZFHX3 overexpression was associated with a significant increase in mammosphere forming efficiency and the population size of ALDH<sup>+</sup>/CD44<sup>+</sup>/CD24<sup>-</sup> cells (Figure 2d–f). These results imply that ZFHX3 is required for maintaining BCSC-like properties of breast cancer cells in vitro.

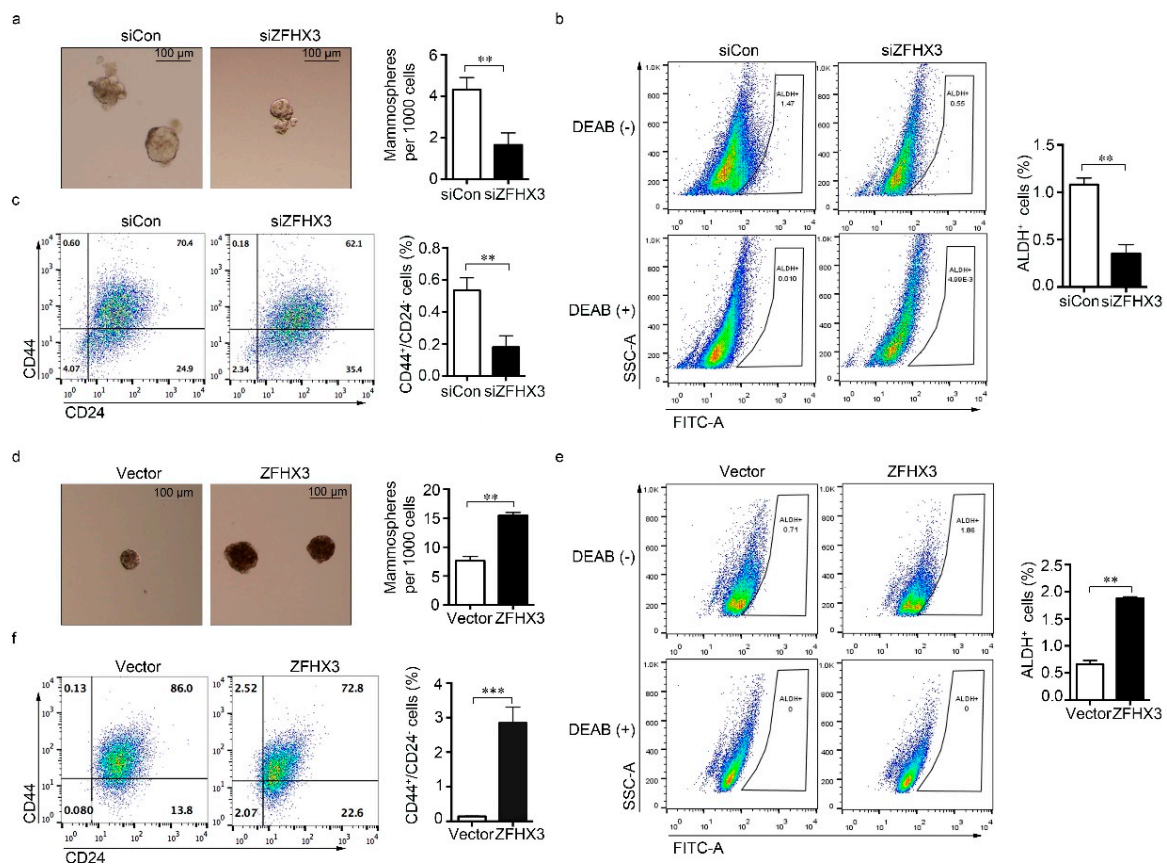


**Figure 2.** ZFH3 maintains stem-like characteristics of ER<sup>+</sup> MCF-7 and T-47D breast cancer cells. (a–c) RNAi-mediated knockdown of ZFH3 in MCF-7 cells decreased mammosphere forming ability (a), as indicated by images of mammospheres (left) and their quantification (right) from the mammosphere formation assay, and the populations of ALDH<sup>+</sup> (b) and CD44<sup>+</sup>/CD24<sup>-</sup> (c) cells, as analyzed by flow cytometry. (d–f) Ectopic expression of ZFH3 in T-47D cells increased mammosphere forming ability (d) and the populations of ALDH<sup>+</sup> (e) and CD44<sup>+</sup>/CD24<sup>-</sup> (f) cells, as analyzed by flow cytometry. siCon, control siRNA; siZFHX3, siRNA against ZFH3. \*\*  $p < 0.01$ ; \*\*\*  $p < 0.001$ . The blank and isotype controls are shown in Supplementary Figure S6.

### 2.3. ZFH3 Upregulates Stemness Factors Including MYC and TBX3 in Breast Cancer Cells

To further investigate the role of ZFH3 in the maintenance of BCSC characteristics and explore the underlying mechanisms, we analyzed whether ZFH3 modulates the expression of multiple pluripotency factors and stemness markers, including MYC, TBX3, OCT4, NANOG, and SOX2, which are involved in the acquisition and maintenance of stem cell properties [27–32]. We first detected four of the five stemness factors in xenograft tumors from T-47D cells ectopically expressing ZFH3 by IHC staining. Overexpression of ZFH3 significantly increased the ratio of positive cells for each of the four factors (Figure 3a,b). Consistently, western blotting showed that ectopic expression of Flag-tagged ZFH3 in T-47D cells upregulated MYC, TBX3, OCT4, NANOG, and SOX2 (Figure 3c). In MCF-7 cells, ZFH3 silencing by RNAi decreased the expression of MYC and TBX3 as well as that of OCT4, NANOG, and SOX2 (Figure 3d). Thus, the promotion of BCSC properties by ZFH3 might involve the enhanced expression of stemness factors.

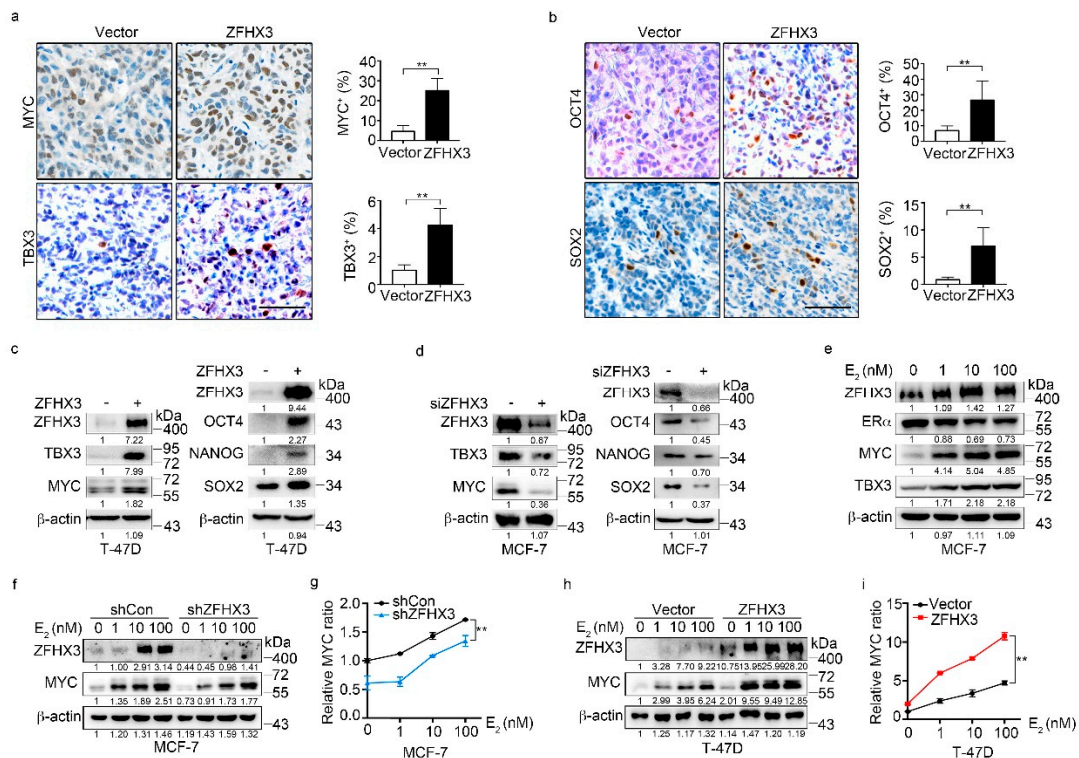


**Figure 3.** ZFH3 induces the expression of MYC and TBX3 in ER<sup>+</sup> MCF-7 and T-47D breast cancer cells. (a,b) Detection of MYC, TBX3, OCT4, and SOX2 by IHC staining in xenograft tumors of T-47D cells ectopically expressing ZFH3, as shown by representative IHC images (left) and quantification of cells with positive staining (right). Scale bar, 50  $\mu$ m. (c,d) Ectopic expression of ZFH3 in T-47D cells increased (c), while ZFH3 silencing in MCF-7 cells decreased (d), the expression of MYC, TBX3, OCT4, NANOG, and SOX2, as detected by western blotting analysis. (e) Estrogen (E<sub>2</sub>) increased MYC and TBX3 in MCF-7 cells, as detected by western blotting. (f–i) ZFH3 silencing in MCF-7 cells attenuated, while ectopic expression of ZFH3 in T-47D cells enhanced, E<sub>2</sub>-mediated MYC expression, as detected by western blotting (f,h) and quantified by relative MYC ratio (g,i). Cells were treated with E<sub>2</sub> for 24 h at the indicated concentrations. siCon, control siRNA; siZFH3, siRNA against ZFH3. \*\* *p* < 0.01. (a,b) IHC staining was done in xenograft tumors. (c–i) cells were cultured in 2D plastic surface and examined with western blotting. Ratios of protein band intensities to those of their loading controls, with the control sample’s normalized to 1, are shown under western blot bands (c–f,h). Uncropped western blot images are available in Supplementary Figure S8.

Among these factors, MYC and TBX3 are particularly interesting, because they have been well implicated in BCSC features and breast carcinogenesis [33,34]. TBX3 also promotes mammary epithelial cell stemness and the initiation and progression of breast cancer [28,35]. We, therefore, analyzed the effect of ZFH3 on the expression of MYC and TBX3. ZFH3 silencing in BT-474 and T-47D cells downregulated MYC and TBX3 expression as expected (Figure S5). In MCF-7 cells, estrogen treatment increased ZFH3 and MYC expression in a dose-dependent manner, while the effect was less evident for TBX3 (Figure 3e). Based on the dose-dependent correlation between ZFH3 and MYC expression (Figure 3e) and MYC is a well-known estrogen-induced gene, we then examined whether estrogen-induced MYC expression requires ZFH3. In MCF-7 cells treated with estrogen, which induced dose-dependent upregulation of both ZFH3 and MYC, knockdown of ZFH3 decreased MYC expression compared to the control group (Figure 3f,g). Consistently, ectopic expression of ZFH3 in T-47D cells further increased estrogen-induced MYC expression compared to the vector control (Figure 3h,i). Estrogen still increased MYC expression in a dose-dependent manner in both MCF-7 cells with ZFH3 silencing and T-47D cells with ZFH3 overexpression (Figure 3f–i), suggesting that estrogen signaling and ZFH3 are two independent events in MYC regulation.

#### 2.4. ZFH3 Transactivates MYC and TBX3 in Breast Cancer Cells

ZFH3 is a transcription factor, so we investigated whether ZFH3 directly transactivates MYC and TBX3. Real-time qPCR showed that MYC and TBX3 mRNAs were decreased by silencing ZFH3 in MCF-7 cells (Figure 4a) and were increased by ectopic expression of Flag-tagged ZFH3 in T-47D cells (Figure 4b).

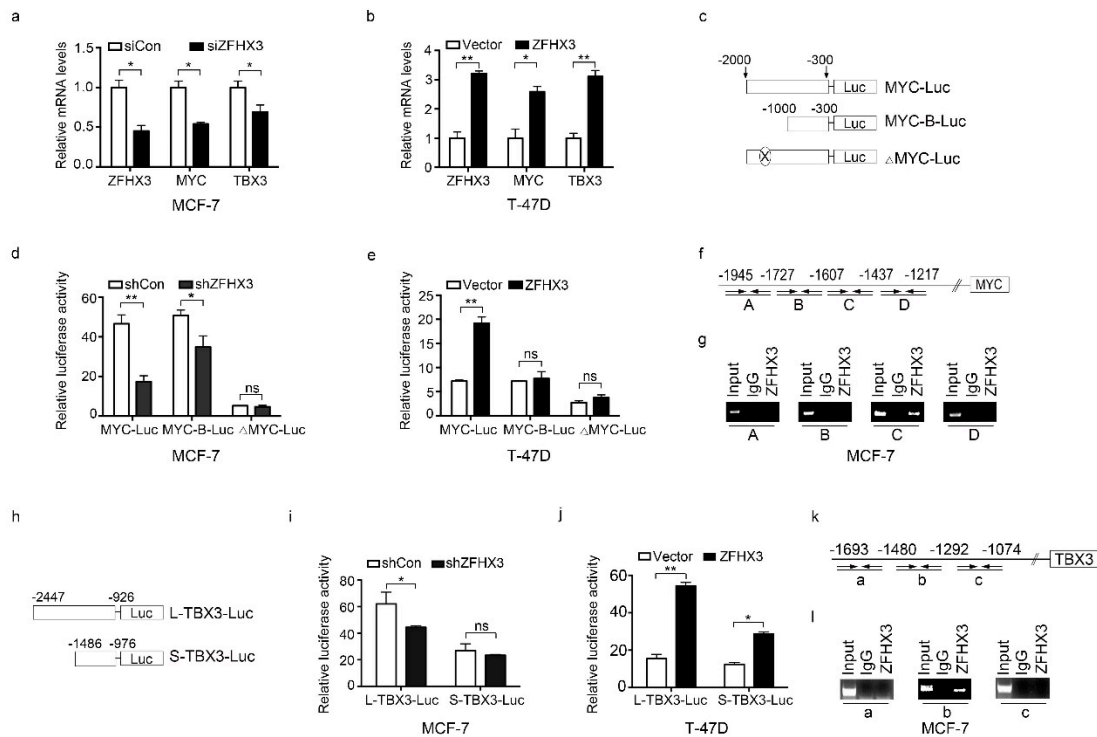


**Figure 4.** ZFH3 activates MYC and TBX3 transcription by binding to their promoters in ER<sup>+</sup> MCF-7 and T-47D breast cancer cells. (a,b) ZFH3 silencing in MCF-7 cells decreased, while ectopic expression of ZFH3 in T-47D (b) cells increased, mRNA levels of MYC and TBX3, as detected by real-time PCR. (c) Schematic for the construction of different MYC promoter-luciferase reporter plasmids. MYC-Luc, 2 kb promoter sequences; MYC-B-Luc, 1 kb; ΔMYC-Luc, the 171 bp from −1607 to −1437 bp upstream to the transcription initiation site was deleted. (d,e) ZFH3 silencing in MCF-7 cells (d) and ZFH3 expression in T-47D cells (e) had different effects on the activities of different MYC promoter constructs, as detected by luciferase reporter assay. (f,g) Location of PCR primer pairs, indicated by arrows, that define fragments A, B, C, and D in the MYC promoter (f) and detection of ZFH3 binding to the C region (−1607 to −1437 bp) by ChIP-PCR. (h) Schematic for the construction of TBX3 promoter-reporter plasmids. L-TBX3-Luc and S-TBX3-Luc contain 1.52 kb and 0.51 kb DNA sequence, respectively, upstream to the TBX3 transcription initiation site. (i,j) Effects of ZFH3 silencing in MCF-7 cells (i) and ZFH3 expression in T-47D cells (j) on the two TBX3 constructs' luciferase activities, as detected by luciferase reporter assay. (k,l) Location of PCR primer pairs, indicated by arrows, that define fragments a, b, and c in the TBX3 promoter (k) and detection of ZFH3 binding to the b region (−1480 to −1292 bp) by ChIP-PCR (l). siCon, control siRNA; siZFHX3, siRNA against ZFH3. ns, not significant; \*  $p < 0.05$ ; \*\*  $p < 0.01$ . Cells were cultured on a 2D plastic surface, then examined in real-time PCR, promoter-luciferase assay, and ChIP assay.

We then conducted a luciferase promoter-reporter assay to test the effect of ZFH3 on MYC promoter activity. MYC promoters of two sizes, one 2 kb, and the other 1 kb upstream to the transcription initiation site, were cloned into the pGL3-Basic luciferase reporter vector for analysis (Figure 4c). ZFH3 silencing in MCF-7 cells decreased MYC promoter activity for both constructs, particularly the longer one (Figure 4d). Ectopic expression of ZFH3 in T-47D cells increased MYC

promoter activity for the longer one but not for the shorter one (Figure 4e), suggesting that ZFH3 acts on the distal site of the *MYC* promoter.

Indeed, the deletion of fragment C from 1607 to −1437 bp in the distal region of the *MYC* promoter (Figure 4c) prevented ZFH3 from inducing *MYC* promoter activity in both MCF-7 and T-47D cells (Figure 4d,e). To test whether ZFH3 binds to the *MYC* promoter, the chromatin immunoprecipitation (ChIP) assay was performed in MCF-7 cells with four sets of primers spanning four fragments (A, B, C, D) of the distal region of *MYC* promoter between −2000 and −1000 bp (Figure 4f). Compared to the control IgG, only fragment C of the promoter from −1607 to −1437 bp was detected in ZFH3-bound DNA (Figure 4g). Therefore, ZFH3 directly binds to an element in the 171 bp DNA of the *MYC* promoter's distal region to activate *MYC* transcription.

We also analyzed whether ZFH3 directly activates *TBX3* transcription. Two fragments of the *TBX3* promoter were cloned into the pGL3-Basic luciferase reporter plasmid (Figure 4h, L-TBX3 and S-TBX3), and a luciferase activity assay was performed. RNAi-mediated ZFH3 silencing in MCF-7 cells decreased the longer promoter's activity but not that of the shorter one (Figure 4i), while ZFH3 overexpressed in T-47D cells increased the activities of both the longer and shorter promoters (Figure 4j). Using the same chromatin precipitates pulled down by the ZFH3 antibody or its control IgG, PCR with three pairs of primers amplifying three fragments of the *TBX3* promoter region from −1693 to −1074 bp (Figure 4k) demonstrated that fragment b (from −1480 to −1292 bp) was present in ZFH3-bound DNA, but fragments a and c were not (Figure 4l). These results suggest that ZFH3 also binds to the *TBX3* promoter to activate its transcription.

### 2.5. Roles of *MYC* and *TBX3* in BCSC Features in the Context of ZFH3 Expression

We further tested whether the upregulation of *MYC* and *TBX3* by ZFH3 has functional significance in BCSC properties by analyzing sphere formation and ALDH<sup>+</sup> cell populations. As expected for established functions of *MYC* and *TBX3* in BCSC regulation, overexpression of *MYC* or *TBX3* alone significantly increased sphere formation efficiency in both MCF-7 and T-47D cells and induced the ALDH<sup>+</sup> population in T-47D cells. In T-47D cells overexpressing ZFH3, both *MYC* and *TBX3* were upregulated (Figure 3c), sphere formation was increased, and *MYC* silencing decreased sphere formation in both vector control and ZFH3 overexpressing cells (Figure 5a,b). In MCF-7 cells with ZFH3 silencing, which downregulated both *MYC* and *TBX3* (Figure 3d) and reduced sphere formation (Figure 2a), ectopic expression of *MYC* failed to increase sphere formation, although it still significantly increased sphere formation in the control group (Figure 5c,d), suggesting that *MYC* restoration alone is not enough to overcome the effect of ZFH3 silencing on spheres.

Sphere formation was also analyzed for *TBX3*, and similar results were obtained. In T-47D cells with ectopic expression of ZFH3, knockdown of *TBX3* dramatically reduced spheres in both the control and ZFH3 groups, and the effect of ZFH3 expression was not detectable after *TBX3* knockdown (Figure 5e,f). In MCF-7 cells with ZFH3 silencing, *TBX3* expression significantly increased spheres in the siRNA control group, and the effect was not statistically significant in the ZFH3 silencing group as well (Figure 5g,h), suggesting that *TBX3* alone is also limited in rescuing the effect of ZFH3 silencing on sphere formation.

The ALDH<sup>+</sup> cell population was also analyzed. In MCF-7 cells with ZFH3 silencing, which significantly reduced the percentage of ALDH<sup>+</sup> cells, expression of *TBX3* increased the ALDH<sup>+</sup> population, but the increase did not completely rescue the effect of ZFH3 silencing (Figure 5i). The expression of *MYC* had even a weaker effect than did *TBX3*, even though the expression of either *MYC* or *TBX3* significantly increased the ALDH<sup>+</sup> population in the siRNA control group (Figure 5i). In T-47D cells with ectopic expression of ZFH3, the ALDH<sup>+</sup> population was significantly increased. Silencing either *MYC* or *TBX3* by RNAi decreased the ALDH<sup>+</sup> population in both the vector control and ZFH3 groups, but neither eliminated the effect of ZFH3 (Figure 5j). Therefore, it appears that both *MYC* and *TBX3* are involved in ZFH3 maintained BCSC properties.



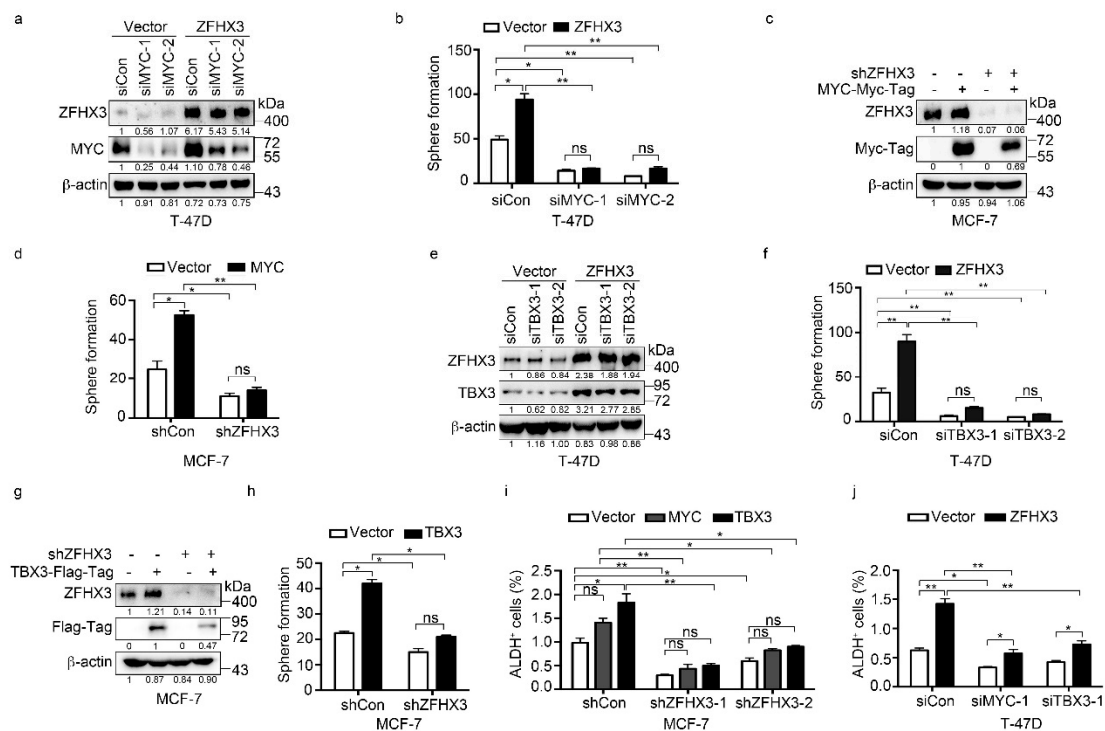


**Figure 5.** MYC and TBX3 play a role in ZFH3-mediated sphere formation in Matrigel and ALDH<sup>+</sup> cell population in ER<sup>+</sup> MCF-7 and T-47D breast cancer cells. (a,b) In T-47D cells ectopically expressing ZFH3, MYC silencing, as confirmed by western blotting in 2D culture (a), and culture in Matrigel (3D culture) that attenuated sphere formation in both ZFH3 and vector control groups (b). (c,d) In MCF-7 cells with ZFH3 silencing, MYC ectopic expression, as confirmed by western blotting in 2D culture (c), and culture in Matrigel (3D culture) that did not significantly increase sphere number (d). (e,f) In T-47D cells ectopically expressing ZFH3, TBX3 silencing, as confirmed by western blotting in 2D culture (e), and culture in Matrigel (3D culture) that attenuated sphere formation (f). (g,h) In MCF-7 cells with ZFH3 silencing, TBX3 ectopic expression, as confirmed by western blotting in 2D culture (g), and culture in Matrigel (3D culture) that did not significantly increase sphere number (h). (i,j) ALDH<sup>+</sup> cells were then detected by flow cytometry in MCF-7 cells with ZFH3 silencing and MYC or TBX3 overexpression (i) and T-47D cells with ZFH3 overexpression and MYC or TBX3 knockdown (j). ns, not significant; \* *p* < 0.05; \*\* *p* < 0.01. Cells were cultured on a 2D plastic surface. siCon, control siRNA; siZFH3, siRNA against ZFH3. Ratios of protein band intensities to those of their loading controls, with the control sample's normalized to 1, are shown under western blot bands (a,c,e,g). Uncropped western blot images are available in Supplementary Figure S9.

### 3. Discussion

In this study, we examined the role of ZFH3 in the regulation of breast cancer growth and potential underlying mechanisms. We report that ZFH3 enhances cell proliferation and tumor growth of ER<sup>+</sup> breast cancer cells. Such a pro-proliferative function involves an enhanced breast cancer stemness and transcriptional upregulation of two factors that have a well-established role in breast cancer, MYC and TBX3.

ZFH3 has been suspected of playing a role in breast carcinogenesis because it interacts with ER and PR to regulate gene expression, cell proliferation, cell differentiation, and mammary gland development [15,20]. Both ER and PR have been well implicated in breast cancer. However, direct evidence for such a role of ZFH3 has been lacking. Our findings in this study indicate that ZFH3 plays a promoting role in breast cancer, as its knockdown attenuated, while its ectopic expression promoted, the proliferation and tumorigenicity of breast cancer cells in both in vitro and in vivo models (Figure 1 and Figure S2). ZFH3 also enhanced breast cancer stemness, as indicated by ZFH3-induced

increases in mammosphere formation and the populations of ALDH<sup>+</sup> or CD44<sup>+</sup>/CD24<sup>-</sup> cells (Figure 2), and cancer stemness is crucial for tumor initiation and progression. A promoting effect of ZFHX3 on breast cancer is further supported by the correlation of higher *ZFHX3* expression levels with worse patient survival in breast cancer patients of the TCGA database (Figure 1i).

We noticed that ZFHX3 is a tumor suppressor in prostate cancer, as it is frequently mutated in advanced diseases, and its deletion induces or promotes prostatic carcinogenesis in mice [36–38]. Even in breast cancer, a tumor suppressor activity has been suggested, as higher levels of the longer transcript of *ZFHX3* (*ZFHX3-A*) correlate with markers of better prognosis such as negative lymph node involvement, lower tumor grade, and smaller tumor size [17]; and in ER<sup>+</sup>/PR<sup>+</sup> breast cancer cell lines MCF-7 and T-47D cultured in a hormone-free medium, ZFHX3 was inhibitory to estrogen-mediated cell proliferation in 2D culture [20]. These findings appear to contradict the observed tumor-promoting effect of ZFHX3 in this study.

The reasons for such inconsistencies are unknown but are likely very complicated. For example, the two splicing variants of *ZFHX3* (*ZFHX3-A* and *ZFHX3-B*) could have different functions under different contexts, even though we used *ZFHX3-A* in the ectopic expression experiments. The correlation between *ZFHX3* mRNA expression and the better prognosis was restricted to the *ZFHX3-A* transcript [17]. However, our analysis of TCGA data, where the splicing variants of *ZFHX3* cannot be distinguished, showed that higher levels of *ZFHX3* mRNA expression correlated with worse patient survival (Figure 1i). In the BreastMark database, higher levels of *ZFHX3* mRNA is also associated with poor survival in breast cancer patients [39]. The notion of the two splicing forms having different functions is speculative and remains to be tested.

Interactions of ZFHX3 with other proteins could also modulate protein SUMOylation [40] and regulate multiple pathophysiological processes such as development [15,16,41] and tumorigenesis [37,38]. Such interactions could also make ZFHX3 function in a context-dependent manner. For example, ZFHX3 promotes liver cancer cells' tumor growth by interacting with HIF1A to enhance angiogenesis [42]. More directly, SUMOylation of ZFHX3 at lysine 2806 is essential for its tumor-promoting effect on the tumorigenicity of MDA-MB-231 cells, as the mutation of lysine 2806 in ZFHX3 prevented MDA-MB-231 cells from forming tumors in nude mice [43].

A more plausible explanation is that ZFHX3 is anti-proliferative when only the estrogen signaling is activated but becomes pro-proliferative when both the estrogen and progesterone signaling is activated. This notion originated from our previous studies of *Zfhx3* in mouse mammary gland development at different stages. *Zfhx3* modulates multiple hormonal signaling pathways, including estrogen, progesterone, and prolactin [15,16,20,37]. In pubertal mammary glands, estrogen is the primary hormone driving gland development. In such glands, the deletion of *Zfhx3* enhances ductal elongation and bifurcation and promotes the proliferation of ER-positive cells [14]. It thus appears that *Zfhx3* inhibits the proliferation of mammary epithelial cells when only the estrogen signaling is activated. However, in mature mammary glands, both the estrogen and progesterone signaling is activated, and in such glands, the deletion of *Zfhx3* suppresses side-branching, alveologenesis and cell proliferation [15]. It is noteworthy that only when both estrogen and progesterone are present does *Zfhx3* promote cell proliferation, as seen in mice with ovariectomy and supplement of estrogen and/or progesterone [15]. Therefore, *Zfhx3* exerts contradicting roles in the proliferation of normal mammary epithelial cells, being pro-proliferative when both estrogen and progesterone are present but anti-proliferative when estrogen is dominant.

In our previous study, where ZFHX3 inhibited the proliferation of breast cancer cells [20], cells were cultured in the hormone-free medium for three days to eliminate the effect of other hormones. After that, only the estrogen was added to the medium for analysis [20]. Such a scenario is more analogous to pubertal mammary glands (only the estrogen is dominant), and ZFHX3 being anti-proliferative could thus be expected. In our current study, cells were cultured in a complete medium containing multiple growth factors and hormones and are thus more analogous to adult mammary glands (both estrogen and progesterone are present). ZFHX3's pro-proliferative function in such a scenario could be

expected. Therefore, the role of ZFH3 in breast cancer appears to be context-dependent. How ZFH3 executes such a context-dependent function is an important but unanswered question.

Enhancing stemness via transcriptional activation of multiple stem cell factors is a possible mechanism for ZFH3 to promote breast cancer cells' proliferation and tumor growth. Flow cytometry analysis demonstrated that ZFH3 was involved in maintaining the populations of CD44<sup>+</sup>/CD24<sup>-</sup> and ALDH<sup>+</sup> cells, both highly enriched for BCSCs and thus have been used to identify BCSCs [44–47]. ZFH3 silencing decreased, while ectopic expression of ZFH3 increased, both cell populations (Figure 2) and mammosphere formation (Figure 2). In mammary epithelial cells, ZFH3 appeared to regulate the expansion of progenitor cells [19] and deletion of *Zfh3* in mouse mammary epithelial cells attenuates side-branching and alveologenesis, which involve active proliferation of mammary stem cells [15]. Therefore, although enhanced breast cancer stemness could be a cellular mechanism that is partially responsible for the tumor-promoting effect of ZFH3 in breast cancer, a firm role of ZFH3 in the maintenance of BCSCs remains to be established.

Molecularly, MYC and TBX3 could be partially responsible for ZFH3's promoting cell proliferation and tumor growth effects. Among the five stem cell markers tested, MYC and TBX3 were more highly induced by ZFH3 (Figure 3). Indeed, ZFH3 bound to their promoters to activate their transcription (Figure 4), and re-analysis of the ChIP-seq data from previous studies [16,48,49] using the ChipEnrich program also supported a direct binding of ZFH3 to the MYC promoter. Direct binding of ZFH3 to MYC promoter has also been detected in prostate cancer cells [50]. Both MYC and TBX3 play important roles in breast cancer and BCSCs. MYC is a potent oncogene that alone can reactivate the embryonic stem cell-like program in normal and cancer cells [29,33,51–55] that is overexpressed by various mechanisms in more than half of breast cancers [33,56–59]; and functionally, MYC indeed contributes to tumor initiation and progression in breast cancer [33,34,60]. At least for MYC, its expression levels correlate with the extents of its effect on cell proliferation. TBX3 is a T-box transcription factor that increases FGF secretion and Wnt signaling activity in mammary glands [61] to regulate self-renewal and differentiation of stem cells [35,62]. TBX3 modulates early embryo and mammary gland development [63,64] and breast cancer initiation and progression via multiple mechanisms such as the paracrine FGF/FGFR/TBX3 signaling pathway [28,35,65–68]. Breast tumors with higher TBX3 expression levels have greater recurrence rates [64,69]. We should mention that OCT4, NANOG, and SOX2 could also explain the effect of ZFH3 on BCSC features as they are known stem cell factors, and their expression was also upregulated by ZFH3 in breast cancer cells (Figure 3).

Although MYC and TBX3 could partially mediate ZFH3's promoting effects on cell proliferation and tumor growth, direct evidence is still lacking at this time because findings from the rescue experiments were not conclusive (Figure 5). In T-47D cells where MYC or TBX3 silencing dramatically reduced sphere colony formation, ectopic expression of ZFH3 showed a trend of increasing sphere formation, but the increase was not statistically significant (Figure 5a,b,e,f). On the other hand, in MCF-7 cells where ZFH3 silencing significantly decreased sphere formation and MYC and TBX3 downregulation, re-expression of MYC or TBX3 showed a trend of increasing sphere formation. Still, again the increase was not statistically significant. Multiple reasons could be responsible for these inclusive findings. For example, other molecules could mediate ZFH3's function. In T-47D cells, ZFH3 is likely only one of several factors that upregulate MYC and TBX3; RNAi-mediated silencing of MYC or TBX3 could be too potent.

## 4. Materials and Methods

### 4.1. Cell Lines and Cell Culture

Human breast cancer cell lines MCF-7, T-47D, BT-474, and MDA-MB-231 cells were obtained from ATCC (Manassas, VA, USA). MCF-7 cells were cultured in Dulbecco's modified Eagle's medium (DMEM) (Gibco, Grand Island, NY, USA) supplemented with 10% fetal bovine serum (FBS; Gibco).

T-47D, BT-474, and MDA-MB-231 cells were cultured in RPMI-1640 medium (Gibco) supplemented with 10% FBS. Cells were cultured at 37 °C with 5% CO<sub>2</sub>. The immortalized non-tumorigenic human breast epithelial cell line MCF10A was purchased from ATCC and cultured in DMEM/F12 medium supplemented with 5% horse serum, 20 ng/mL epidermal growth factor (EGF), 10 µg/mL insulin, 0.5 µg/mL hydrocortisone, and 100 ng/mL cholera toxin.

In experiments involving treatment of cells with estrogen, which was purchased from Sigma-Aldrich (St. Louis, MO, USA), ER<sup>+</sup> breast cancer cells were cultured in phenol red-free medium supplemented with 5% charcoal dextran-stripped FBS for 24 h, and estrogen was added.

#### 4.2. RNA Extraction and Quantitative Real-Time RT-PCR

Total RNA was extracted using the TRIzol reagent (Invitrogen, Carlsbad, CA, USA), and cDNA was synthesized with the MMLV-Reverse Transcriptase system (Promega, Madison, WI, USA). Real-time PCR was performed with the Mastercycler ep realplex system (Eppendorf, Hamburg, Germany) using the SYBR premix Ex Taq (TaKaRa, Tokyo, Japan). RNA expression levels were normalized to glyceraldehyde-3-phosphate dehydrogenase (GAPDH). PCR primers used are shown in Supplementary Table S1.

#### 4.3. RNA Interference

Cells were seeded onto 6-well plates, grown to 60–80% confluency, and then transfected with small interfering RNAs (siRNAs) using the Lipofectamine RNAiMAX (Invitrogen) according to the manufacturer's instructions. The siRNA against *ZFH3*, which targets both *ZFH3-A* and *ZFH3-B*, was from a previous study [20]. Sequences for siRNAs are: GGAACUAUGACCUCGACUATT (siMYC-1); GAACACACAACGUCUUGGATT (siMYC-2); CCUGGAGGCUAAAGAACUUTT (siTBX3-1); and GCCUCCACUGUAGGGACAUTT (siTBX3-2).

#### 4.4. Western Blotting

Cells were washed with PBS and lysed using SDS Lysis buffer (P1016, Solarbio, Beijing, China). Cell lysates containing equal amounts of proteins were separated by 4% (for *ZFH3*) or 10% (for all other proteins) SDS-PAGE, then transferred to polyvinylidene fluoride (PVDF) membranes (Millipore, Billerica, MA, USA). The membranes were blocked with 5% nonfat milk at room temperature for 2 h and probed with primary antibodies at 4 °C overnight, then incubated with secondary antibodies for 2 h at room temperature. They were then visualized using WesternBright ECL (Advansta, Menlo Park, CA, USA), and protein signals were detected with the luminescent Image Analyzer (Jun Yi Dong Fang, Beijing, China). Protein band intensities were determined using the ImageJ program and ratios of protein band intensities to those of their loading controls were calculated as previously described [70]. *ZFH3*, whose molecular weight is 404 KDa, and the antibody for *ZFH3* has been described in our previous study [20]. Other antibodies included β-actin (1:8000, 3700, Cell Signaling, Danvers, MA, USA); MYC (1:1000, 9402, Cell Signaling); TBX3 (1:1000, ab154828, Abcam, Cambridge, MA, USA); OCT4 (1:1000, 2750, Cell Signaling); NANOG (1:1000, 4903, Cell Signaling); SOX2 (1:1000, ab92494, Abcam); ERα (1:1000, sc-53493, Santa Cruz, CA, USA); FLAG (1:3000, SAB4200071, Sigma); and Myc-Tag (1:500, 06-549, Sigma). Original unedited blots can be found at Supplementary Figure S7–S12.

#### 4.5. Establishment of Cell Lines

MISSION<sup>TM</sup> shRNAs targeting *ZFH3* in pLKO.1-puro plasmid and vector control plasmid were purchased from Sigma. Lentiviral particles were produced in 293T cells by cotransfecting pLKO.1 with pMD2.G and psPAX2 plasmids using the FuGENE 6 transfection reagent according to the manufacturer's protocol (Promega). MCF-7 cells were seeded in 6-well plates and cultured with fresh medium containing 8 µg/mL of Polybrene (Sigma), and 1 mL of lentiviral solution was added dropwise. After 6 h of viral infection, the virus-containing medium was replaced with a fresh medium containing puromycin at 2 µg/mL (Sigma) for 3 days to select cells stably expressing shRNAs. MCF-7 cells expressing

shZFHX3 were maintained in a medium containing 1 µg/mL puromycin. Sequences of shRNAs against ZFHX3 are CCGGGCCAGGAAGAATTATGAGAATCTCGAGATTCTCATAATTCTTCTGGCTTTTT (shZFHX3-1) and CCGGCCCTTTAGTTTCCACAGCTAACTCGAGTTAGCTGTGGAACTAAAGGGT TTTT (shZFHX3-2), which have been previously described [16].

T-47D cells were transfected with pcDNA3.0-Flag, and Flag-tagged ZFHX3 using the Lipofectamine 2000 Transfection Reagent (Invitrogen), and transfected cells were selected with 1 mg/mL G418 for 14 days. ZFHX3 expression in transfected T-47D cells was confirmed by western blotting.

#### 4.6. Cell Growth and Proliferation Assay

Cell growth and proliferation were analyzed by the sulforhodamine B (SRB) staining assay. MCF-7 cells were seeded onto 24-well plates and transfected with siRNAs against ZFHX3 or control. T-47D cells were seeded on 24-well plates and transfected with pcDNA3.0-Flag or Flag-tagged ZFHX3. The culture medium was replaced every other day. At desired time points, cells were fixed by 10% trichloroacetic acid (TCA) for 1 h at 4 °C, stained with 0.4% SRB (Sigma), and washed with 1% acetic acid. Stained cells were dissolved, and the absorbance was measured.

#### 4.7. Sphere Formation Assay in Matrigel (3D Culture)

The growth factor reduced Matrigel (354230, Corning, NY, USA) was used for this assay. Briefly, cells were seeded onto 6-well plates and transfected with siRNA or plasmids. Eight-well chamber slides (PEZGS0896, Millipore) were loaded with 40 µL Matrigel, solidified at 37 °C for at least 30 min. A total of 2500 (Figure 1) or 1000 (Figure 5) treated cells in the mixture of medium containing 10% FBS and 2% Matrigel were overlaid on the gel and were then grown for 2 weeks, with the medium renewed every 2 days. Images of spheres were subjected to the ImageJ computer program [70] to determine the spheres' diameter and number.

#### 4.8. Mammosphere Formation Assay

A single-cell suspension was obtained and plated in ultra-low attachment plates (3471, Corning) at a density of 1000 cells per well. Cells were then cultured in a complete mammosphere culture medium (05620, Stem Cell Technology, Vancouver, BC, Canada) for 10–14 days. The number of mammospheres with a diameter >60 µm was determined using the Image J program.

#### 4.9. Flow Cytometry Assay

A single-cell suspension was washed with phosphate-buffered saline (PBS), resuspended in PBS (10<sup>6</sup> cells per 100 µL), and incubated with the antibodies of human cell surface markers PE-CD24 (560991, BD Pharmingen, San Diego, CA, USA) and APC-CD44 (559942, BD Pharmingen) for 1 h on ice in the dark. Control samples were incubated with isotype-matched control IgG, PE-anti-CD24 (555574, BD Pharmingen), APC-anti-CD44 (555745, BD Pharmingen) for 1 h on ice in the dark. Unbound antibodies were washed off, and labeled cells were analyzed using the BD FACS-Calibur (BD Biosciences, San Jose, CA, USA).

#### 4.10. Aldefluor Assay

The Aldefluor assay was performed using the Aldefluor kit from Stem Cell Technology following the manufacturer's protocol (01700, Stem Cell Technology). Briefly, 10<sup>6</sup> cells were resuspended in 1 mL Aldefluor buffer, and 5 µL of ALDH substrate (BAAA) was added and mixed. 500 µL of the cell suspension was immediately transferred to another tube containing 5 µL of diethylaminobenzaldehyde (DEAB), an ALDH inhibitor, mixed evenly, and used as the negative control. Cells in both tubes were incubated for 40 min at 37 °C, washed, resuspended in 500 µL Aldefluor buffer, and then analyzed with the BD FACS-Calibur (BD Biosciences).

#### 4.11. Promoter-Luciferase Assay

Cells were seeded in 24-well plates, cultured overnight, and then transfected with the promoter-reporter plasmids using the Lipofectamine 2000 Transfection Reagent (Invitrogen). After 48 h, cells were collected in reporter lysis buffer (E3971, Promega), and the luciferase activity was measured using the dual-luciferase assay kit (Promega) with a luminometer ((Tristar LB941, Berthold Technologies, BadWild, Germany). Primer sequences for cloning the promoters of *MYC* and *TBX3* are listed in Supplementary Table S1.

#### 4.12. Chromatin Immunoprecipitation (ChIP) Assay

ChIP assays were performed by using the Simple ChIP Enzymatic Chromatin Immunoprecipitation Kit (9003, Cell Signaling Technology) according to the manufacturer's instructions. ChIP products were detected by regular PCR. Primer sequences for *MYC* and *TBX3* promoters are shown in Table S1.

#### 4.13. Tumorigenesis Assay

T-47D cells stably transfected with Flag-tagged vector or Flag-ZFH3 plasmid were resuspended in PBS/Matrigel (354234, Corning) at 1: 1 ratio and injected into the inguinal mammary gland of BALB/c nu/nu athymic mice (4–6-week-old female) ( $n = 6$ ) at  $5 \times 10^6$  cells per gland, with the vector control cells injected into the right side mammary fat pad and Flag-ZFH3 cells into the left mammary fat pad. Estrogen pellets were implanted in the back of the neck. For Supplementary Figure 2,  $1 \times 10^7$  MCF-7 cells of shZFH3 or control (shCon) were suspended in 100  $\mu$ L of PBS/Matrigel (354234, Corning) mix (1:1) and injected subcutaneously into mammary fat pads of female nude mice. Estrogen pellets were implanted into the back of the neck. The length (L) and width (W) of xenograft tumors were measured once a week. At the end of the experiment, mice were euthanized; and tumors were isolated, fixed in 4% paraformaldehyde, and subjected to IHC or hematoxylin and eosin (HE) staining.

#### 4.14. Immunohistochemical (IHC) Staining

Fixed tumors were paraffin-embedded and sectioned, and sections were deparaffinized, rehydrated following standard procedure, and IHC staining was performed with an IHC kit from MXB (KT-5001, Fuzhou, Fujian, China). Tissue sections were then stained with hematoxylin, dehydrated, and mounted. In T-47D cells with ZFH3 overexpressing, ZFH3 was localized in both the cytoplasm and nucleus (Figure 1h), whereas Ki67, MYC, TBX3, OCT4, and SOX2 were localized in the nucleus (Figure 3a,b). For the quantification of ZFH3 expression, slides were scanned using an Aperio VERSA 8 Scanner System (Leica Microsystems, Wetzlar, Germany). The ImageJ program was then used to determine the intensity of positively stained signal (brown) and the total nuclei (blue) in the tissue area. The average intensity per nucleus (cell) was then calculated. For the other five proteins, images of stained tissue sections were taken at 20 $\times$  magnification using either the same Aperio VERSA 8 system or an Aperio ScanScope XT system (Leica). The numbers of positively stained cells and total cells were then determined from 3–5 images using the ImageJ program. The ratio of positively stained cells to total cells was used for comparison.

The antibodies used in IHC analysis included ZFH3 (1:1000, PD010, MBL, Nagoya Aichi, Japan), Ki67 (1:2000, ab15580, Abcam), MYC (1:1000, ab32072, Abcam), TBX3 (1:100, SRP08533, Tianjin Saierbio, Tianjin, China), OCT4 (1:1000, 2750, Cell Signaling), and SOX2 (1:1000, ab92494, Abcam).

#### 4.15. Bioinformatic and Survival Analyses

Gene expression profile of GSE15192 was downloaded from the Gene Expression Omnibus (GEO) [71,72] and applied for heat-map via R language software (Windows v3.6.3, <https://www.r-project.org/>). Correlation of survival with different expression levels of ZFH3 in patients with breast cancer was analyzed and visualized by the embedded UALCAN tool in the TCGA database [21,22].

#### 4.16. Statistical Analysis

All in vitro experiments were repeated at least twice. Statistical analyses were performed using the SPSS statistical software (SPSS, Version 20; IBM, Armonk, NY, USA). Two-tailed Student's *t*-test was used to compare two groups, and one-way ANOVA was used for comparison of more than two groups. All quantitative data are expressed as mean  $\pm$  SD. *p* values less than 0.05 were considered statistically significant.

### 5. Conclusions

In summary, these findings suggest that transcription factor ZFH3 plays a promoting function in breast cancer cells' proliferation and tumor growth involving the BCSC properties. Molecularly, ZFH3 could bind to the promoters of *MYC* and *TBX3* to activate their transcription, which could then partially mediate ZFH3's effects on cell proliferation and tumor growth. These findings thus suggest a novel molecular mechanism underlying breast carcinogenesis that could help develop therapeutic strategies for the treatment of breast cancer.

**Supplementary Materials:** The following are available online at <http://www.mdpi.com/2072-6694/12/11/3415/s1>, Figure S1: Expression of ZFH3, MYC, and TBX3 in breast cell lines; Figure S2: ZFH3 silencing in MCF-7 breast cancer cells attenuates tumor growth; Figure S3: Association of ZFH3 expression with those of BCSC markers in different populations of MCF10A cells; Figure S4: Stable knockdown of ZFH3 attenuates stem cell features in MCF-7 cells; Figure S5: ZFH3 silencing reduces MYC and TBX3 expression in BT-474 and T-47D cells; Figure S6: The blank and isotype controls for the flow cytometry analysis; Figure S7: Uncropped western blot images for Figure 1; Figure S8: Uncropped western blot images for Figure 3; Figure S9: Uncropped western blot images for Figure 5; Figure S10: Uncropped western blot images for Figure S1; Figure S11: Uncropped western blot images for Figure S4; Figure S12: Uncropped western blot images for Figure S5, Table S1: Primer sequences.

**Author Contributions:** Data curation, J.L. and X.L. (Xiawei Li); Funding acquisition and overall supervision, J.-T.D.; Investigation, G.D., G.M., R.W., J.L., M.L., A.G., X.L. (Xiawei Li), and J.A.; Methodology, G.M.; Project administration, L.F.; Writing—original draft, G.D.; Writing—review and editing, X.L. (Xiaoyu Liu), Z.Z., B.Z., and J.-T.D. All authors have read and agreed to the published version of the manuscript.

**Funding:** This work was supported by a grant from the National Natural Science Foundation of China, grant number 31871466.

**Acknowledgments:** We thank Anthea Hammond for editing the manuscript and Qingxia Hu and Yuyang Qian for help during the study.

**Conflicts of Interest:** All authors declare no conflict of interest in this work.

### References

1. Siegel, R.L.; Miller, K.D.; Jemal, A. Cancer statistics, 2020. *CA Cancer J. Clin.* **2020**, *70*, 7–30. [[CrossRef](#)] [[PubMed](#)]
2. Perou, C.M.; Sorlie, T.; Eisen, M.B.; Van de Rijn, M.; Jeffrey, S.S.; Rees, C.A.; Pollack, J.R.; Ross, D.T.; Johnsen, H.; Akslen, L.A.; et al. Molecular portraits of human breast tumours. *Nature* **2000**, *406*, 747–752. [[CrossRef](#)] [[PubMed](#)]
3. Sorlie, T.; Perou, C.M.; Tibshirani, R.; Aas, T.; Geisler, S.; Johnsen, H.; Hastie, T.; Eisen, M.B.; Van de Rijn, M.; Jeffrey, S.S.; et al. Gene expression patterns of breast carcinomas distinguish tumor subclasses with clinical implications. *Proc. Natl. Acad. Sci. USA* **2001**, *98*, 10869–10874. [[CrossRef](#)]
4. Weigelt, B.; Mackay, A.; A'Hern, R.; Natrajan, R.; Tan, D.S.; Dowsett, M.; Ashworth, A.; Reis-Filho, J.S. Breast cancer molecular profiling with single sample predictors: A retrospective analysis. *Lancet Oncol.* **2010**, *11*, 339–349. [[CrossRef](#)]
5. Creighton, C.J.; Kent Osborne, C.; Van de Vijver, M.J.; Foekens, J.A.; Klijn, J.G.; Horlings, H.M.; Nuyten, D.; Wang, Y.; Zhang, Y.; Chamness, G.C.; et al. Molecular profiles of progesterone receptor loss in human breast tumors. *Breast Cancer Res. Treat.* **2009**, *114*, 287–299. [[CrossRef](#)] [[PubMed](#)]
6. Ismail, P.M.; Amato, P.; Soyal, S.M.; DeMayo, F.J.; Conneely, O.M.; O'Malley, B.W.; Lydon, J.P. Progesterone involvement in breast development and tumorigenesis—as revealed by progesterone receptor “knockout” and “knockin” mouse models. *Steroids* **2003**, *68*, 779–787. [[CrossRef](#)]

7. Obr, A.E.; Edwards, D.P. The biology of progesterone receptor in the normal mammary gland and in breast cancer. *Mol. Cell. Endocrinol.* **2012**, *357*, 4–17. [[CrossRef](#)]
8. Chatterton, R.T., Jr.; Lydon, J.P.; Mehta, R.G.; Mateo, E.T.; Pletz, A.; Jordan, V.C. Role of the progesterone receptor (PR) in susceptibility of mouse mammary gland to 7,12-dimethylbenz[a]anthracene-induced hormone-independent preneoplastic lesions in vitro. *Cancer Lett.* **2002**, *188*, 47–52. [[CrossRef](#)]
9. Briskin, C. Progesterone signalling in breast cancer: A neglected hormone coming into the limelight. *Nat. Rev. Cancer* **2013**, *13*, 385–396. [[CrossRef](#)]
10. Mohammed, H.; Russell, I.A.; Stark, R.; Rueda, O.M.; Hickey, T.E.; Tarulli, G.A.; Serandour, A.A.; Birrell, S.N.; Bruna, A.; Saadi, A.; et al. Progesterone receptor modulates ERalpha action in breast cancer. *Nature* **2015**, *523*, 313–317. [[CrossRef](#)]
11. Miura, Y.; Tam, T.; Ido, A.; Morinaga, T.; Miki, T.; Hashimoto, T.; Tamaoki, T. Cloning and characterization of an ATBF1 isoform that expresses in a neuronal differentiation-dependent manner. *J. Biol. Chem.* **1995**, *270*, 26840–26848. [[CrossRef](#)] [[PubMed](#)]
12. Ido, A.; Miura, Y.; Tamaoki, T. Activation of ATBF1, a multiple-homeodomain zinc-finger gene, during neuronal differentiation of murine embryonal carcinoma cells. *Dev. Biol.* **1994**, *163*, 184–187. [[CrossRef](#)] [[PubMed](#)]
13. Jung, C.G.; Kim, H.J.; Kawaguchi, M.; Khanna, K.K.; Hida, H.; Asai, K.; Nishino, H.; Miura, Y. Homeotic factor ATBF1 induces the cell cycle arrest associated with neuronal differentiation. *Development* **2005**, *132*, 5137–5145. [[CrossRef](#)] [[PubMed](#)]
14. Li, M.; Fu, X.; Ma, G.; Sun, X.; Dong, X.; Nagy, T.; Xing, C.; Li, J.; Dong, J.T. Atbf1 regulates pubertal mammary gland development likely by inhibiting the pro-proliferative function of estrogen-ER signaling. *PLoS ONE* **2012**, *7*, e51283. [[CrossRef](#)]
15. Ma, G.; Gao, A.; Yang, Y.; He, Y.; Zhang, X.; Zhang, B.; Zhang, Z.; Li, M.; Fu, X.; Zhao, D.; et al. Zfhx3 is essential for progesterone/progesterone receptor signaling to drive ductal side-branching and alveologenesis in mouse mammary glands. *J. Genet. Genom.* **2019**, *46*, 119–131. [[CrossRef](#)]
16. Zhao, D.; Ma, G.; Zhang, X.; He, Y.; Li, M.; Han, X.; Fu, L.; Dong, X.Y.; Nagy, T.; Zhao, Q.; et al. Zinc finger homeodomain factor Zfhx3 is essential for mammary lactogenic differentiation by maintaining prolactin signaling activity. *J. Biol. Chem.* **2016**, *291*, 12809–12820. [[CrossRef](#)]
17. Zhang, Z.; Yamashita, H.; Toyama, T.; Sugiura, H.; Ando, Y.; Mita, K.; Hamaguchi, M.; Kawaguchi, M.; Miura, Y.; Iwase, H. ATBF1-A messenger RNA expression is correlated with better prognosis in breast cancer. *Clin. Cancer Res.* **2005**, *11*, 193–198.
18. Dong, X.Y.; Guo, P.; Sun, X.; Li, Q.; Dong, J.T. Estrogen up-regulates ATBF1 transcription but causes its protein degradation in estrogen receptor-alpha-positive breast cancer cells. *J. Biol. Chem.* **2011**, *286*, 13879–13890. [[CrossRef](#)]
19. Li, M.; Zhao, D.; Ma, G.; Zhang, B.; Fu, X.; Zhu, Z.; Fu, L.; Sun, X.; Dong, J.T. Upregulation of ATBF1 by progesterone-PR signaling and its functional implication in mammary epithelial cells. *Biochem. Biophys. Res. Commun.* **2013**, *430*, 358–363. [[CrossRef](#)]
20. Dong, X.Y.; Sun, X.; Guo, P.; Li, Q.; Sasahara, M.; Ishii, Y.; Dong, J.T. ATBF1 inhibits estrogen receptor (ER) function by selectively competing with AIB1 for binding to the ER in ER-positive breast cancer cells. *J. Biol. Chem.* **2010**, *285*, 32801–32809. [[CrossRef](#)]
21. UALCAN. Available online: <http://ualcan.path.uab.edu/> (accessed on 8 May 2019).
22. Chandrashekar, D.S.; Bashel, B.; Balasubramanya, S.A.H.; Creighton, C.J.; Ponce-Rodriguez, I.; Chakravarthi, B.; Varambally, S. UALCAN: A Portal for Facilitating Tumor Subgroup Gene Expression and Survival Analyses. *Neoplasia* **2017**, *19*, 649–658. [[CrossRef](#)] [[PubMed](#)]
23. Al-Hajj, M.; Wicha, M.S.; Benito-Hernandez, A.; Morrison, S.J.; Clarke, M.F. Prospective identification of tumorigenic breast cancer cells. *Proc. Natl. Acad. Sci. USA* **2003**, *100*, 3983–3988. [[CrossRef](#)] [[PubMed](#)]
24. Phillips, T.M.; McBride, W.H.; Pajonk, F. The response of CD24(-/low)/CD44+ breast cancer-initiating cells to radiation. *J. Natl. Cancer Inst.* **2006**, *98*, 1777–1785. [[CrossRef](#)]
25. Ponti, D.; Costa, A.; Zaffaroni, N.; Pratesi, G.; Petrangolini, G.; Coradini, D.; Pilotti, S.; Pierotti, M.A.; Daidone, M.G. Isolation and in vitro propagation of tumorigenic breast cancer cells with stem/progenitor cell properties. *Cancer Res.* **2005**, *65*, 5506–5511. [[CrossRef](#)]



26. Bhat-Nakshatri, P.; Appaiah, H.; Ballas, C.; Pick-Franke, P.; Goulet, R., Jr.; Badve, S.; Srour, E.F.; Nakshatri, H. SLUG/SNAI2 and tumor necrosis factor generate breast cells with CD44+/CD24- phenotype. *BMC Cancer* **2010**, *10*, 411. [[CrossRef](#)] [[PubMed](#)]
27. Eilers, M.; Eisenman, R.N. Myc's broad reach. *Genes Dev.* **2008**, *22*, 2755–2766. [[CrossRef](#)]
28. Fillmore, C.M.; Gupta, P.B.; Rudnick, J.A.; Caballero, S.; Keller, P.J.; Lander, E.S.; Kuperwasser, C. Estrogen expands breast cancer stem-like cells through paracrine FGF/Tbx3 signaling. *Proc. Natl. Acad. Sci. USA* **2010**, *107*, 21737–21742. [[CrossRef](#)]
29. Kim, J.; Woo, A.J.; Chu, J.; Snow, J.W.; Fujiwara, Y.; Kim, C.G.; Cantor, A.B.; Orkin, S.H. A Myc network accounts for similarities between embryonic stem and cancer cell transcription programs. *Cell* **2010**, *143*, 313–324. [[CrossRef](#)] [[PubMed](#)]
30. Lu, X.; Mazur, S.J.; Lin, T.; Appella, E.; Xu, Y. The pluripotency factor nanog promotes breast cancer tumorigenesis and metastasis. *Oncogene* **2014**, *33*, 2655–2664. [[CrossRef](#)]
31. Luo, W.; Li, S.; Peng, B.; Ye, Y.; Deng, X.; Yao, K. Embryonic stem cells markers SOX2, OCT4 and Nanog expression and their correlations with epithelial-mesenchymal transition in nasopharyngeal carcinoma. *PLoS ONE* **2013**, *8*, e56324. [[CrossRef](#)]
32. Wong, D.J.; Segal, E.; Chang, H.Y. Stemness, cancer and cancer stem cells. *Cell Cycle* **2008**, *7*, 3622–3624. [[CrossRef](#)] [[PubMed](#)]
33. Liao, D.J.; Dickson, R.B. c-Myc in breast cancer. *Endocr. Relat. Cancer* **2000**, *7*, 143–164. [[CrossRef](#)] [[PubMed](#)]
34. Pelengaris, S.; Khan, M.; Evan, G. c-MYC: More than just a matter of life and death. *Nat. Rev. Cancer* **2002**, *2*, 764–776. [[CrossRef](#)] [[PubMed](#)]
35. Dong, L.; Lyu, X.; Faleti, O.D.; He, M.L. The special stemness functions of Tbx3 in stem cells and cancer development. *Semin. Cancer Biol.* **2019**, *57*, 105–110. [[CrossRef](#)]
36. Sun, X.; Frierson, H.F.; Chen, C.; Li, C.; Ran, Q.; Otto, K.B.; Cantarel, B.L.; Vessella, R.L.; Gao, A.C.; Petros, J.; et al. Frequent somatic mutations of the transcription factor ATBF1 in human prostate cancer. *Nat. Genet.* **2005**, *37*, 407–412. [[CrossRef](#)]
37. Sun, X.; Fu, X.; Li, J.; Xing, C.; Frierson, H.F.; Wu, H.; Ding, X.; Ju, T.; Cummings, R.D.; Dong, J.T. Deletion of Atbf1/Zfhx3 in mouse prostate causes neoplastic lesions, likely by attenuation of membrane and secretory proteins and multiple signaling pathways. *Neoplasia* **2014**, *16*, 377–389. [[CrossRef](#)]
38. Sun, X.; Xing, C.; Fu, X.; Li, J.; Zhang, B.; Frierson, H.F.J.; Dong, J.T. Additive effect of Zfhx3/Atbf1 and Pten deletion on mouse prostatic tumorigenesis. *J. Genet. Genom.* **2015**, *42*, 373–382. [[CrossRef](#)]
39. Madden, S.F.; Clarke, C.; Gaule, P.; Aherne, S.T.; O'Donovan, N.; Clynes, M.; Crown, J.; Gallagher, W.M. BreastMark: An integrated approach to mining publicly available transcriptomic datasets relating to breast cancer outcome. *Breast Cancer Res.* **2013**, *15*, R52. [[CrossRef](#)]
40. Sun, X.; Li, J.; Dong, F.N.; Dong, J.T. Characterization of nuclear localization and SUMOylation of the ATBF1 transcription factor in epithelial cells. *PLoS ONE* **2014**, *9*, e92746. [[CrossRef](#)]
41. Sun, X.; Fu, X.; Li, J.; Xing, C.; Martin, D.W.; Zhang, H.H.; Chen, Z.; Dong, J.T. Heterozygous deletion of Atbf1 by the Cre-loxP system in mice causes preweaning mortality. *Genesis* **2012**, *50*, 819–827. [[CrossRef](#)]
42. Fu, C.; An, N.; Liu, J.; Jun, A.; Zhang, B.; Liu, M.; Zhang, Z.; Fu, L.; Tian, X.; Wang, D.; et al. The transcription factor ZFH3 is crucial for the angiogenic function of hypoxia-inducible factor 1 $\alpha$  in liver cancer cells. *J. Biol. Chem.* **2020**, in press. [[CrossRef](#)]
43. Wu, R.; Fang, J.; Liu, M.; Jun, A.; Liu, J.; Chen, W.; Li, J.; Ma, G.; Zhang, Z.; Zhang, B.; et al. SUMOylation of the transcription factor ZFH3 at Lys-2806 requires SAE1, UBC9, and PIAS2 and enhances its stability and function in cell proliferation. *J. Biol. Chem.* **2020**, *295*, 6741–6753. [[CrossRef](#)] [[PubMed](#)]
44. Sheridan, C.; Kishimoto, H.; Fuchs, R.K.; Mehrotra, S.; Bhat-Nakshatri, P.; Turner, C.H.; Goulet, R., Jr.; Badve, S.; Nakshatri, H. CD44+/CD24- breast cancer cells exhibit enhanced invasive properties: An early step necessary for metastasis. *Breast Cancer Res.* **2006**, *8*, R59. [[CrossRef](#)] [[PubMed](#)]
45. Ginestier, C.; Hur, M.H.; Charafe-Jauffret, E.; Monville, F.; Dutcher, J.; Brown, M.; Jacquemier, J.; Viens, P.; Kleer, C.G.; Liu, S.; et al. ALDH1 is a marker of normal and malignant human mammary stem cells and a predictor of poor clinical outcome. *Cell Stem Cell* **2007**, *1*, 555–567. [[CrossRef](#)] [[PubMed](#)]
46. Li, W.; Ma, H.; Zhang, J.; Zhu, L.; Wang, C.; Yang, Y. Unraveling the roles of CD44/CD24 and ALDH1 as cancer stem cell markers in tumorigenesis and metastasis. *Sci. Rep.* **2017**, *7*, 13856. [[CrossRef](#)] [[PubMed](#)]

47. Ricardo, S.; Vieira, A.F.; Gerhard, R.; Leitão, D.; Pinto, R.; Cameselle-Teijeiro, J.F.; Milanezi, F.; Schmitt, F.; Paredes, J. Breast cancer stem cell markers CD44, CD24 and ALDH1: Expression distribution within intrinsic molecular subtype. *J. Clin. Pathol.* **2011**, *64*, 937–946. [[CrossRef](#)]
48. Yan, J.; Enge, M.; Whittington, T.; Dave, K.; Liu, J.; Sur, I.; Schmierer, B.; Jolma, A.; Kivioja, T.; Taipale, M.; et al. Transcription factor binding in human cells occurs in dense clusters formed around cohesin anchor sites. *Cell* **2013**, *154*, 801–813. [[CrossRef](#)] [[PubMed](#)]
49. Welch, R.P.; Lee, C.; Imbriano, P.M.; Patil, S.; Weymouth, T.E.; Smith, R.A.; Scott, L.J.; Sartor, M.A. ChIP-Enrich: Gene set enrichment testing for ChIP-seq data. *Nucleic Acids Res.* **2014**, *42*, e105. [[CrossRef](#)]
50. Hu, Q.; Zhang, B.; Chen, R.; Fu, C.; Jun, A.; Fu, X.; Li, J.; Fu, L.; Zhang, Z.; Dong, J.T. ZFH3 is indispensable for ER $\beta$  to inhibit cell proliferation via MYC downregulation in prostate cancer cells. *Oncogenesis* **2019**, *8*, 28. [[CrossRef](#)]
51. Takahashi, K.; Yamanaka, S. Induction of pluripotent stem cells from mouse embryonic and adult fibroblast cultures by defined factors. *Cell* **2006**, *126*, 663–676. [[CrossRef](#)]
52. Park, I.H.; Zhao, R.; West, J.A.; Yabuuchi, A.; Huo, H.; Ince, T.A.; Lerou, P.H.; Lensch, M.W.; Daley, G.Q. Reprogramming of human somatic cells to pluripotency with defined factors. *Nature* **2008**, *451*, 141–146. [[CrossRef](#)] [[PubMed](#)]
53. Dang, C.V. Have you seen...?: Micro-managing and restraining pluripotent stem cells by MYC. *EMBO J.* **2009**, *28*, 3065–3066. [[CrossRef](#)] [[PubMed](#)]
54. Nie, Z.; Hu, G.; Wei, G.; Cui, K.; Yamane, A.; Resch, W.; Wang, R.; Green, D.R.; Tessarollo, L.; Casellas, R.; et al. c-Myc is a universal amplifier of expressed genes in lymphocytes and embryonic stem cells. *Cell* **2012**, *151*, 68–79. [[CrossRef](#)] [[PubMed](#)]
55. Wong, D.J.; Liu, H.; Ridky, T.W.; Cassarino, D.; Segal, E.; Chang, H.Y. Module map of stem cell genes guides creation of epithelial cancer stem cells. *Cell Stem Cell* **2008**, *2*, 333–344. [[CrossRef](#)]
56. Agnantis, N.J.; Mahera, H.; Maounis, N.; Spandidos, D.A. Immunohistochemical study of ras and myc oncoproteins in apocrine breast lesions with and without papillomatosis. *Eur. J. Gynaecol. Oncol.* **1992**, *13*, 309–315.
57. Saccani Jotti, G.; Fontanesi, M.; Bombardieri, E.; Gabrielli, M.; Veronesi, P.; Bianchi, M.; Becchi, G.; Bogni, A.; Tardini, A. Preliminary study on oncogene product immunohistochemistry (c-erbB-2, c-myc, ras p21, EGFR) in breast pathology. *Int. J. Biol. Markers* **1992**, *7*, 35–42. [[CrossRef](#)]
58. Hehir, D.J.; McGreal, G.; Kirwan, W.O.; Kealy, W.; Brady, M.P. c-myc oncogene expression: A marker for females at risk of breast carcinoma. *J. Surg. Oncol.* **1993**, *54*, 207–209. [[CrossRef](#)]
59. Spaventi, R.; Kamenjicki, E.; Pecina, N.; Grazio, S.; Grazio, S.; Pavelic, J.; Kusic, B.; Cvrtila, D.; Danilovic, Z.; Spaventi, S.; et al. Immunohistochemical detection of TGF- $\alpha$ , EGF-R, c-erbB-2, c-H-ras, c-myc, estrogen and progesterone in benign and malignant human breast lesions: A concomitant expression. *In Vivo* **1994**, *8*, 183–189.
60. Wang, Y.H.; Liu, S.; Zhang, G.; Zhou, C.Q.; Zhu, H.X.; Zhou, X.B.; Quan, L.P.; Bai, J.F.; Xu, N.Z. Knockdown of c-Myc expression by RNAi inhibits MCF-7 breast tumor cells growth in vitro and in vivo. *Breast Cancer Res.* **2005**, *7*, R220–R228. [[CrossRef](#)]
61. Eblaghie, M.C.; Song, S.J.; Kim, J.Y.; Akita, K.; Tickle, C.; Jung, H.S. Interactions between FGF and Wnt signals and Tbx3 gene expression in mammary gland initiation in mouse embryos. *J. Anat.* **2004**, *205*, 1–13. [[CrossRef](#)]
62. Jiang, K.; Ren, C.; Nair, V.D. MicroRNA-137 represses Klf4 and Tbx3 during differentiation of mouse embryonic stem cells. *Stem Cell Res.* **2013**, *11*, 1299–1313. [[CrossRef](#)] [[PubMed](#)]
63. Washkowitz, A.J.; Gavrilov, S.; Begum, S.; Papaioannou, V.E. Diverse functional networks of Tbx3 in development and disease. *Wiley Interdiscip. Rev. Syst. Biol. Med.* **2012**, *4*, 273–283. [[CrossRef](#)] [[PubMed](#)]
64. Khan, S.F.; Damerell, V.; Omar, R.; Du Toit, M.; Khan, M.; Maranyane, H.M.; Mlaza, M.; Bleloch, J.; Bellis, C.; Sahm, B.D.B.; et al. The roles and regulation of TBX3 in development and disease. *Gene* **2020**, *726*, 144223. [[CrossRef](#)] [[PubMed](#)]
65. Douglas, N.C.; Papaioannou, V.E. The T-box transcription factors TBX2 and TBX3 in mammary gland development and breast cancer. *J. Mammary Gland Biol. Neoplasia* **2013**, *18*, 143–147. [[CrossRef](#)]
66. Krstic, M.; Macmillan, C.D.; Leong, H.S.; Clifford, A.G.; Souter, L.H.; Dales, D.W.; Postenka, C.O.; Chambers, A.F.; Tuck, A.B. The transcriptional regulator TBX3 promotes progression from non-invasive to invasive breast cancer. *BMC Cancer* **2016**, *16*, 671. [[CrossRef](#)]

67. Liu, J.; Esmailpour, T.; Shang, X.; Gulsen, G.; Liu, A.; Huang, T. TBX3 over-expression causes mammary gland hyperplasia and increases mammary stem-like cells in an inducible transgenic mouse model. *BMC Dev. Biol.* **2011**, *11*, 65. [[CrossRef](#)]
68. Yarosh, W.; Barrientos, T.; Esmailpour, T.; Lin, L.; Carpenter, P.M.; Osann, K.; Anton-Culver, H.; Huang, T. TBX3 is overexpressed in breast cancer and represses p14 ARF by interacting with histone deacetylases. *Cancer Res.* **2008**, *68*, 693–699. [[CrossRef](#)]
69. Dong, L.; Dong, Q.; Chen, Y.; Li, Y.; Zhang, B.; Zhou, F.; Lyu, X.; Chen, G.G.; Lai, P.; Kung, H.F.; et al. Novel HDAC5-interacting motifs of Tbx3 are essential for the suppression of E-cadherin expression and for the promotion of metastasis in hepatocellular carcinoma. *Signal Transduct. Target. Ther.* **2018**, *3*, 22. [[CrossRef](#)]
70. Schneider, C.A.; Rasband, W.S.; Eliceiri, K.W. NIH Image to ImageJ: 25 years of image analysis. *Nat Methods* **2012**, *9*, 671–675. [[CrossRef](#)]
71. Gene Expression Omnibus. Available online: <https://www.ncbi.nlm.nih.gov/geo/> (accessed on 20 November 2019).
72. Barrett, T.; Wilhite, S.E.; Ledoux, P.; Evangelista, C.; Kim, I.F.; Tomashevsky, M.; Marshall, K.A.; Phillippy, K.H.; Sherman, P.M.; Holko, M.; et al. NCBI GEO: Archive for functional genomics data sets-update. *Nucleic Acids Res.* **2013**, *41*, D991–D995. [[CrossRef](#)]

**Publisher's Note:** MDPI stays neutral with regard to jurisdictional claims in published maps and institutional affiliations.



© 2020 by the authors. Licensee MDPI, Basel, Switzerland. This article is an open access article distributed under the terms and conditions of the Creative Commons Attribution (CC BY) license (<http://creativecommons.org/licenses/by/4.0/>).